CrossMark

Resonator Stabilization Architecture to Suppress Switching Transient Crosstalk in I-CDM

Malcolm Durkin[1] · **Joel C. Weber[1]** · **William B. Doriese[2]** · **Gene C. Hilton[2]** · **Daniel S. Swetz[2]** · **Joel N. Ullom[1,2]**

Abstract The ever-increasing sizes of transition-edge sensor (TES) microcalorimeter arrays motivates improved multiplexed readout with large multiplexing factors, low power dissipation, and low levels of crosstalk. Current-summed code division multiplexing (I-CDM) has been proposed as an alternative to flux-summed code division multiplexing (Φ-CDM) because of its lower power dissipation and greater robustness against the failure of individual readout elements. Simulating I-CDM arrays, we find that unswitched circuit components provide a mechanism for crosstalk, the magnitude of which is determined by their inductance. To mitigate this source of crosstalk, we propose a technique called resonator-stabilized I-CDM (RI-CDM), which the simulations predict will reduce crosstalk by an order of magnitude. RI-CDM reads out dc-biased TESs on an amplitude-modulated carrier wave.

1 Introduction

Transition-edge sensors (TES) are commonly used for high-performance X-ray microcalorimetry [1, 2] due to their high collecting efficiency and eV-scale energy resolutions. Increasingly large TES arrays are being proposed for X-ray observatory missions [3, 4] and will require advanced superconducting multiplexing techniques. While frequency division multiplexing [5] and microwave SQUID multiplexing [6] techniques are being developed, time division multiplexing (TDM), where each pixel

✉ Malcolm Durkin
  malcolm.durkin@nist.gov

1 University of Colorado Boulder, Boulder, CO, USA

2 National Institute of Standards and Technology, Boulder, CO, USA

is read sequentially, is the most mature readout technique and the dominant technology used in presently deployed TES X-ray calorimeter arrays [7]. Aliased amplifier noise is a key limitation in TDM. In an N-row TDM system, each pixel's first-stage SQUID is only read for $1/N$ of the total measurement time, undersampling the high bandwidth SQUID amplifier and aliasing it by a factor proportional to $\sqrt{N}$ [8]. This noise aliasing limits the multiplexing factors achievable in TDM.

Code division multiplexing (CDM), where TES signals are Walsh-encoded and the sum of the encoded signals is read for the duration of a measurement frame [9], does not suffer from $\sqrt{N}$ noise because all TESs are sampled continuously. Flux-summed CDM [10] (Φ-CDM), where the Walsh codes are hardwired as the polarity of the TES couplings to SQUID flux, is the most advanced type of CDM, with demonstrations of 32 pixel Φ-CDM multiplexers [11]. However, the on-chip wiring complexity required by this technique will likely limit practical implementations to $N_{\text{rows}} \leq 100$.

A proposed alternative CDM technique, current-summed CDM (I-CDM), uses superconducting switches to modulate the polarity of each TES's current signal sent to the input coil of a shared SQUID amplifier [12, 13]. This architecture has the potential advantages of reduced power consumption due to the absence of shunting resistors, more compact layout due to fewer input coils to SQUID amplifiers, and higher chip yield due to simpler wiring. In this paper, we use simulations to assess the feasibility of I-CDM. We identify a mechanism for long-range crosstalk in I-CDM and discuss how to mitigate it.

2 Current-Summed Code Division Multiplexing

An I-CDM circuit schematic is shown in Fig. 1a. A total of N_{rows} TESs are connected in parallel to the input coil of a readout SQUID that is in series with a single transformer (for supplying a voltage, V_{source}). Each TES is in series with its own Nyquist inductor with inductance $L_{\text{Nyq}} \gg t_{\text{frame}} R_{\text{TES}}$ to ensure TES voltage is stable over the duration of a multiplexer readout cycle (frame time). Here, R_{TES} is the resistance of the biased TES and t_{frame} is frame time. Each TES has four superconducting switches to determine the polarity with which the TESs couple to the series combination of the SQUID input coil (switches readout polarity) and the bias transformer (switches polarity with which V_{source} is applied to the TES and Nyquist inductor).

The polarity switches in I-CDM implement a Walsh encoding of the TES current, which is the readout signal of a voltage-biased TES. Depending on the polarity of its switch, a TES makes a positive or negative contribution to the current sent to the input coil of a SQUID. If the TESs have switching patterns that are orthogonal within a readout frame (as shown for four pixels in Fig. 1b), each TES current can be extracted from the summed encoded currents via multiplication by the inverse Walsh code. The four-row encoding in Fig. 1b is used in all simulations presented in this paper.

Each TES's dc voltage bias is obtained by varying V_{source} and modulating the switch polarity so that the Nyquist inductor and the TES receive a nonzero average voltage. Figure 1c shows V_{source}, which has an average of 0 V. TES polarity switching allows a nonzero average voltage bias to be placed across the Nyquist
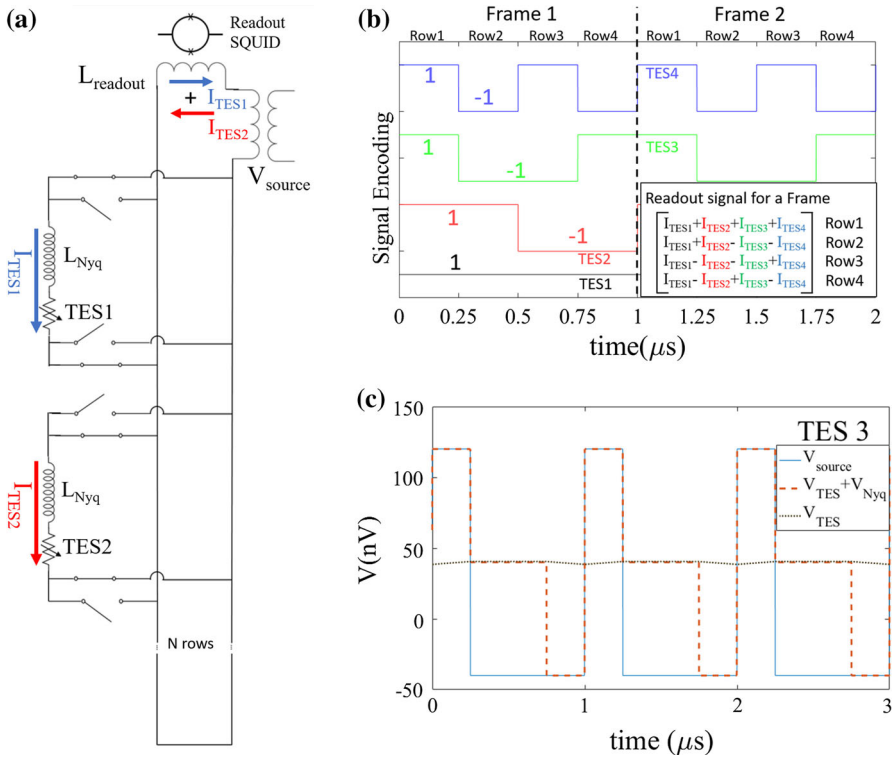
Fig. 1 (Color figure online) *I*-CDM. **a** Circuit diagram of *I*-CDM. **b** A 4-pixel Walsh encoding, which modulates the TES signals by ± 1. After a full readout frame, the signal from each TES can be extracted via multiplication by the inverse Walsh matrix. **c** A voltage, V_{source}, is applied via a transformer. Modulation of the polarity switches allows TES2–4 to be dc-biased at 40 nV. The Nyquist inductor acts as a low-pass filter

inductor and TES ($V_{TES} + V_{Nyq}$). Since $L_{Nyq}/R_{TES} \gg t_{frame}$, the Nyquist inductor filters the applied voltage, resulting in a constant DC voltage bias across the TES (V_{TES}).

Performing simulations in both MATLAB and SPICE, we find that crosstalk arises from voltage spikes that occur when TESs undergo polarity switching events. If the unswitched components (SQUID input coil, bias transformer, and unswitched wires) have a finite inductance ($L_{readout}$), the change in the TES current direction will cause voltage spikes ($V = L \, dI/dt$). We investigate this by simulating a device with $t_{row} = 250$ ns, $R_{sw} = 1.6 \, \Omega$, $L_{nyq} = 1000$ nH, and $L_{readout} = 1$ nH, where t_{row} is row time and R_{sw} is open switch resistance.

These voltage spikes can significantly alter the TES voltage bias even when $L_{Nyq} \gg L_{readout}$. Polarity switches preferentially orient voltage spikes as shown in Fig. 2a, resulting in a net contribution to V_{TES} even when averaged over a measurement frame. Figure 2b and c shows that voltage spikes shift V_{TES} away from the intended value of 40 nV and provide a mechanism for crosstalk (shared $L_{readout}$ allows each TES's switching spikes to affect other TESs). Figure 2b inset shows how switching spikes
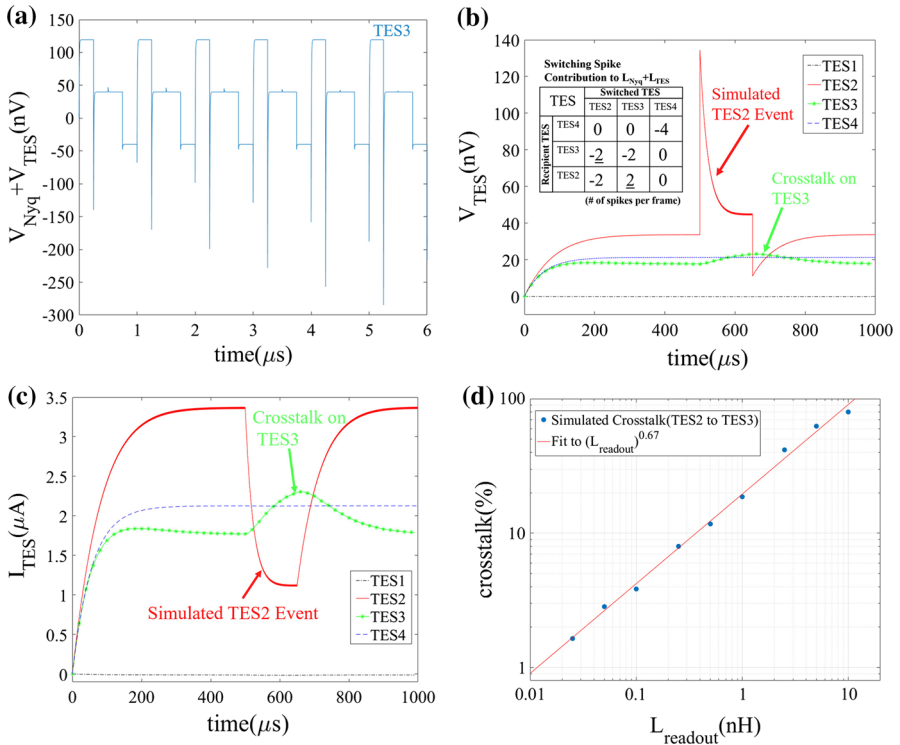
Fig. 2 (Color figure online) *I*-CDM crosstalk. **a** Voltage spikes from row switching events, preferentially oriented downwards, are shown for TES3. From 0 and 200 μs, I_{TES} and V_{TES} are still being ramped up, resulting in increasing spike height. **b** TES bias is shown as a function of time. Switching spikes shift V_{TES} away from 40 nV and provide a mechanism for crosstalk, demonstrated in a simplified TES event (a boxcar function increase in resistance). Inset shows the net contribution each TES's switching event spikes makes to other TESs biases, with crosstalk terms underlined. **c** Crosstalk between TES2 and TES3 is visible in TES currents used for readout. **d** Crosstalk is plotted against $L_{readout}$

from each TES are oriented by recipient TESs, with each spike in a frame time making a 1 or −1 contribution depending on orientation and nonzero numbers indicating a contribution to V_{TES}. In larger arrays, each pixel sends pulses to many others and this mechanism behaves as long-range crosstalk.

To find a practical upper limit for $L_{readout}$, we perform crosstalk simulations on four-pixel *I*-CDM arrays using $t_{row} = 250$ ns, $R_{sw} = 200$ mΩ, $L_{Nyq} = 1000$ nH, and a range of $L_{readout}$ values. Crosstalk is measured as the TES3 response to a TES2 event, plotted against $L_{readout}$ in Fig. 2d. As $L_{readout}$ is decreased, the offset of the voltage bias and the magnitude of the crosstalk also decreases. We find that $L_{readout}$ less than 25 pH is necessary to obtain less than 1% crosstalk in a 4 TES array, which would scale to 0.25% long-range crosstalk in a 16 TES array. Even 0.25% crosstalk for 6-keV TES events results in 15-eV pulses in other channels, which can significantly degrade energy resolution in high-event-rate applications.

(a)
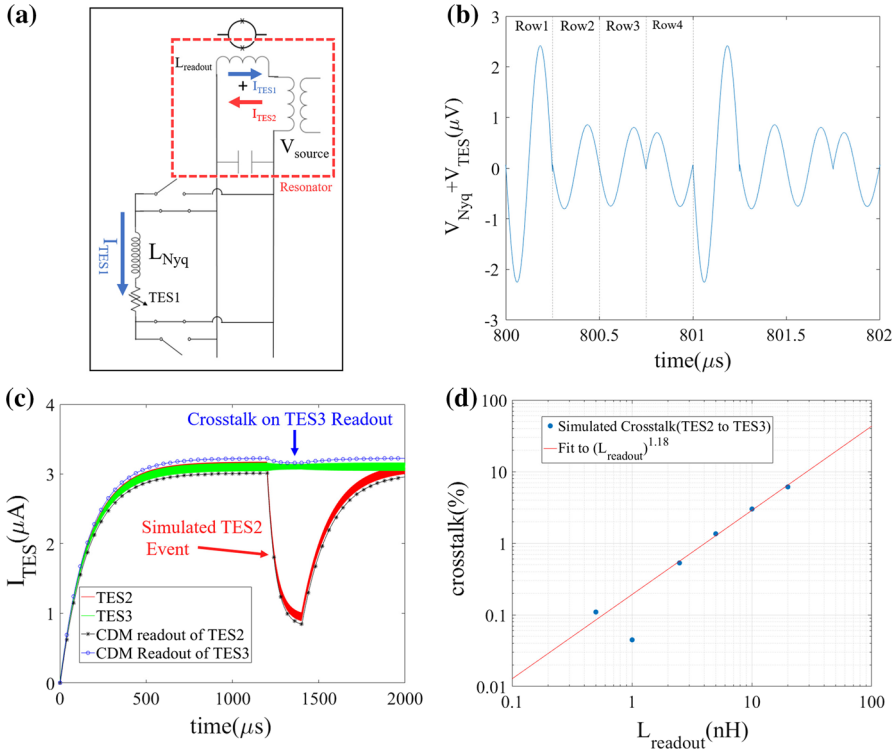

(b)

(c)

(d)

Fig. 3 (Color figure online) Resonator-stabilized I-CDM. **a** A resonator can be created by placing a capacitor in parallel with the polarity-switched TES array. **b** A high-quality factor (Q~31.5) resonator produces a sinusoidal switching transient. The simulations shown involve $R_{sw} = 100\ \Omega$, $L_{Nyq} = 2000$ nH, $L_{readout} = 10$ nH, $C = 159$ nF, and $f_{res} = f_{row} = 4$ MHz. **c** The simulated currents and CDM-extracted currents of TES2 and TES3 are plotted together. **d** Crosstalk as a function of $L_{readout}$, with $C = 1/(L_{readout}\ (2\pi f_{res})^2)$

3 Resonator-Stabilized *I*-CDM

We propose using resonator-stabilized *I*-CDM to reduce crosstalk in *I*-CDM, predicting greater than a factor of 10 reduction for comparable values of $L_{readout}$. As shown in the R*I*-CDM schematic in Fig. 3a, a capacitor is placed in parallel with the readout inductors, forming an underdamped resonator that produces a sinusoidal transient response to a switching event. If the resonant frequency (f_{res}) is an integer multiple of the row frequency (f_{row}) as in Fig. 3b, the TES voltage bias contributions of the negative and positive parts of the sine wave will cancel when averaged over a row time, providing a more stable DC bias. TES currents in Fig. 3c show greatly reduced crosstalk between TES2 and TES3. This trend is demonstrated for a wide range of $L_{readout}$ in Fig. 3d. R*I*-CDM crosstalk reduction improves with greater resonator quality factor, making low $L_{readout}$, high R_{sw}, and large capacitance (C) (and thus, $f_{res} = f_{row}$) favorable.

TES currents in R*I*-CDM can be measured as amplitude-modulated (AM) wave readout signals. The sine wave in the resonator has an amplitude proportional to

the switched current, meaning that TES currents can be obtained by measuring the amplitude of each row and performing CDM operations, with results shown in Fig. 3c.

4 Conclusion and Future Work

Performing simulations to study crosstalk in I-CDM, we identify a crosstalk mechanism that occurs due to switching transients and propose a technique called RI-CDM to reduce it. RI-CDM will require device components that have yet to be developed. Damping limitations require a high-current superconducting switch with $R_{sw} \geq 100\ \Omega$, and fabrication of a compact ~ 160 nF on-chip capacitor is challenging. Development of these devices as well as measurement systems with faster row times would make RI-CDM design considerations more favorable.

References

1. W.B. Doriese, P. Abbamonte, B.L. Alpert, D.A. Bennett, E.V. Denison, Y. Fang, D.A. Fischer, C.P. Fitzgerald, J.W. Fowler, J.D. Gard, J.P. Hays-Wehle, G.C. Hilton, C. Jaye, J.L. McChesney, L. Miaja-Avila, K.M. Morgan, Y.I. Joe, G.C. O'Neil, C.D. Reintsema, F. Rodolakis, D.R. Schmidt, H. Tatsuno, J. Uhlig, L.R. Vale, J.N. Ullom, D.S. Swetz, Rev. Sci. Instrum. **88**, 053108 (2017). https://doi.org/10.1063/1.4983316
2. C.A. Kilbourne, W.B. Doriese, S.R. Bandler, R.P. Brekoskky, A.-D. Brown, J.A. Chervenak, M.E. Eckart, F.M. Finkbeiner, G.C. Hilton, K.D. Irwin, N. Iyomoto, R.L. Kelley, F.S. Porter, C.D. Reintsema, S.J. Smith, J.N. Ullom, Proc SPIE **7011**, 701104 (2008). https://doi.org/10.1117/12790027
3. L. Ravera, D. Barret, J.W. den herder, L. Piro, R. Cledassou, E. Pointecouteau, P. Peille, F. Pajot, M. Arnaud, C. Pigot et al., Proc. SPIE **9144**, 91442L (2014). https://doi.org/10.1117/122055884
4. J.A. Gaskin, M.C. Weisskopf, A. Vikhlinin, H.D. Tananbaum, S.R. Bandler, M.W. Bautz, D.N. Burrows, A.D. Falcone, F.A. Harrison, R.K. Heilmann et al., Proc. SPIE **9601**, 96010J (2015). https://doi.org/10.1117/12.2190837
5. H. Akamatsu, L. Gottardi, C.P. de Vries, J.S. Adams, S.R. Bandler, M.P. Bruijn, J.A. Chervenak, M.E. Eckart, F.M. Finkbeiner, J.R. Gao, J.-W. den Herder, R. den Hartog, H. Hoevers, R.E. Kelley, P. Khosropanah, J. Low Temp. Phys. **184**, 436 (2016). https://doi.org/10.1007/s10909-016-1525-9
6. J.A.B. Mates, D.T. Becker, D.A. Bennet, B.J. Dober, J.D. Gard, J.P. Hays-wehle, J.W. Fowler, G.C. Hilton, C.D. Reintsema, D.R. Schmidt, D.S. Swetz, L.R. Vale, J.N. Ullom, Appl. Phys. Lett. **111**, 062601 (2017). https://doi.org/10.1063/1.4986222
7. W.B. Doriese, K.M. Morgan, D.A. Bennett, E.V. Denison, C.P. Fitzgerald, J.W. Fowler, J.D. Gard, J.P. Hays-Wehle, G.C. Hilton, K.D. Irwin, Y.I. Joe, J.A.B. Mates, G.C. O'Neil, C.D. Reintsema, N.O. Robbins, D.R. Schmidt, D.S. Swetz, H. Tatsuno, L.R. Vale, J.N. Ullom, J. Low Temp. Phys. **184**, 389 (2016). https://doi.org/10.1007/s10909-015-1373-z
8. J. Chervenak, K. Irwin, E. Grossman, J. Martinis, C. Reintsema, M. Huber, Appl. Phys. Lett. **74**, 4043 (1999). https://doi.org/10.1063/1.23255
9. J.L. Walsh, Am. J. Math. **45**, 5 (1923). https://doi.org/10.2307/2387224
10. G.M. Stiehl, W.B. Doriese, J.W. Fowler, G.C. Hilton, K.D. Irwin, C.D. Reintsema, D.R. Schmidt, D.S. Swetz, J.N. Ullom, L.R. Vale, Appl. Phys. Lett. **100**, 072601 (2012). https://doi.org/10.1063/1.3684807
11. K.M. Morgan, B.K. Alpert, D.A. Bennett, E.V. Denison, W.B. Doriese, J.W. Fowler, J.D. Gard, G.C. Hilton, K.D. Irwin, Y.I. Joe, G.C. O'Neil, C.D. Reintsema, D.R. Schmidt, J.N. Ullom, D.S. Swetz, Appl. Phys. Lett. **109**, 112604 (2016). https://doi.org/10.1063/1.4962636

12. K.D. Irwin, H.M. Cho, W.B. Doriese, J.W. Fowler, G.C. Hilton, M.D. Niemack, C.D. Reintsema, D.R. Schmidt, J.N. Ullom, L.R. Vale, J. Low Temp. Phys. **167**, 588 (2012). https://doi.org/10.1007/s10909-012-0586-7
13. M.D. Niemack, J. Beyer, H.M. Cho, W.B. Doriese, G.C. Hilton, K.D. Irwin, C.D. Reintsema, D.R. Schmidt, J.N. Ullom, L.R. Vale, Appl. Phys. Lett. **96**, 163509 (2010). https://doi.org/10.1063/1.3378772